Title

Coordinated Excitation and Inhibition of Prefrontal Ensembles during Awake Hippocampal Sharp-Wave Ripple Events

Journal

Neuron, 90(1)

ISSN

0896-6273

Authors

Jadhav, Shantanu P
Rothschild, Gideon
Roumis, Demetris K
et al.

Publication Date

2016-04-01

DOI

10.1016/j.neuron.2016.02.010

Peer reviewed

HHS Public Access

Author manuscript

Neuron. Author manuscript; available in PMC 2017 April 06.

Published in final edited form as:

Neuron. 2016 April 6; 90(1): 113–127. doi:10.1016/j.neuron.2016.02.010.

Coordinated Excitation and Inhibition of Prefrontal Ensembles During Awake Hippocampal Sharp-Wave Ripple Events

Shantanu P. Jadhav[1,2,*], **Gideon Rothschild**[2,*], **Demetris K. Roumis**[2], and **Loren M. Frank**[2,3]

[1]Neuroscience Program, Department of Psychology and Volen National Center for Complex Systems, Brandeis University, Waltham, U.S.A. (Present address)

[2]Department of Physiology and Center for Integrative Neuroscience, University of California, San Francisco, U.S.A

[3]Howard Hughes Medical Institute

SUMMARY

Interactions between the hippocampus and prefrontal cortex (PFC) are critical for learning and memory. Hippocampal activity during awake sharp wave ripple (SWR) events is important for spatial learning, and hippocampal SWR activity often represents past or potential future experiences. Whether or how this reactivation engages the PFC, and how reactivation might interact with ongoing patterns of PFC activity remains unclear. We recorded hippocampal CA1 and PFC activity in animals learning spatial tasks and found that many PFC cells showed spiking modulation during SWRs. Unlike in CA1, SWR-related activity in PFC comprised both excitation and inhibition of distinct populations. Within individual SWRs, excitation activated PFC cells with representations related to the concurrently reactivated hippocampal representation, while inhibition suppressed PFC cells with unrelated representations. Thus, awake SWRs mark times of strong coordination between hippocampus and PFC that reflects structured reactivation of representations related to ongoing experience.

INTRODUCTION

The hippocampus and medial prefrontal cortex (PFC) play critical roles in storing accounts of experience and retrieving memories to guide future decisions. The hippocampus is necessary for rapid acquisition of memories for new experiences and retrieval of stored

Correspondence: shantanu@brandeis.edu (S.P.J.), loren@phy.ucsf.edu (L.M.F.).
*These authors contributed equally to this work

SUPPLEMENTAL INFORMATION

Supplemental Information includes Supplemental Experimental Procedures, seven figures, and three tables and can be found with this article online.

AUTHOR CONTRIBUTIONS

S.P.J., G.R. and L.M.F. designed the experiments. S.P.J. performed the W-track experiments, and G.R. performed the auditory-cue guided spatial task experiments. S.P.J., G.R., and D.K.R. analyzed the data. L.M.F. supervised all aspects of the data collection and analysis. All authors wrote the paper.

memories during behavior (Squire, 1992; Eichenbaum and Cohen, 2001; Dudai, 2004). The PFC is important for long-term memory storage, memory retrieval, working memory, and decision-making (Hasegawa, 2000; Miller and Cohen, 2001; Sakai, 2003; Wiltgen et al., 2004; Jung et al., 2008; Tse et al., 2011). Moreover, functional disconnection of the hippocampus and PFC causes impairment in some spatial memory tasks (Floresco et al., 1997; Wang and Cai, 2006, 2008). Together, these findings implicate a set of memory functions that rely on both the hippocampus and PFC, but the specific nature of the activity in and communication between these regions that supports memory processes remains unclear.

In the context of memory retrieval, hippocampal – PFC interaction must occur in the awake state and would be expected to reactivate patterns of activity related to behavioral experiences across both structures (Carr et al., 2011; Yu and Frank, 2015). Hippocampal sharp-wave ripple (SWR) events have emerged as a potential mediator of this interaction. During exploration, movement along a spatial trajectory drives the firing of a specific sequence of hippocampal place cells (Skaggs et al., 1996; Dragoi and Buzsaki, 2006). Subsequently, during periods of slow movement and awake immobility, bursts of activity in hippocampal output area CA1 occur in the context of SWRs (Buzsaki, 2015). These bursts often “replay” sequences from behavior (Kudrimoti et al., 1999; Foster and Wilson, 2006; Diba and Buzsaki, 2007; Davidson et al., 2009; Karlsson and Frank, 2009; Gupta et al., 2010; Pfeiffer and Foster, 2013), suggesting that these sequences could support awake memory processes (Carr et al., 2011). Consistent with that possibility, selective disruption of awake SWRs is sufficient to cause a specific learning and memory-guided decision-making deficit (Jadhav et al., 2012).

Do hippocampal SWRs mark the time of coordinated memory reactivation across hippocampus and PFC? This question remains to be answered, but there are a number of results that point to the possibility of such coordination. There are multiple anatomical pathways, including both direct and indirect projections (Amaral and Witter, 1995), that could mediate information flow between the structures. These pathways support memory encoding (Spellman et al., 2015), modulation of hippocampal spatial firing patterns outside of SWRs (Ito et al., 2015), and likely support the observed phase-locking of PFC neurons to the hippocampal theta rhythm seen during movement (Hyman et al., 2005; Jones and Wilson, 2005; Siapas et al., 2005; Benchenane et al., 2010; Gordon, 2011).

Further, while the potential influence of SWRs on PFC during waking behavior has not been examined, previous studies that focused on sleep demonstrated that increases in firing rates of some PFC neurons are seen at the time of SWRs (Wierzynski et al., 2009). Additionally, PFC neurons can reactivate behaviorally-related patterns during sleep (Euston et al., 2007; Peyrache et al., 2009), and this reactivation can coincide with hippocampal SWRs (Peyrache et al., 2009).

At the same time, the possibility of coordinated awake reactivation across hippocampus and PFC raises another question: how does such activity co-exist with ongoing representations of current experience? During the waking state, PFC neurons are known to encode information about task events (Euston et al., 2012), and a subset of PFC neurons are most active during

delays and following receipt of reward (Jung et al., 1998). These are times when SWRs are prominent (Singer and Frank, 2009; Buzsaki, 2015) and it is not clear whether or how SWR-related memory replay and these PFC representations interact.

To determine whether SWRs mark times of coherent memory reactivation across structures and to understand how memory reactivation interacts with ongoing PFC activity, we recorded hippocampal and PFC activity while animals learned spatial tasks. We found coordinated reactivation of activity patterns related to ongoing experience in hippocampal–PFC ensembles during awake SWRs. These findings indicate that awake SWRs are a potential substrate for memory processes.

RESULTS

Excitation and Inhibition of PFC Neurons During Awake Hippocampal SWRs

We used multi-site multi-tetrode drives to simultaneously record the activity of neurons in hippocampus and prefrontal cortex of rats learning either a W-track spatial alternation task (Jadhav et al., 2012), or an auditory cue guided spatial task (n = 3 animals each, Figure 1, see Experimental Procedures). In the W-track alternation task (Figure 1A), animals learned to visit the two outer arms of the W-maze in an alternating sequence, interleaved with visits to the center arm. All animals performed above chance by the 3rd day of training, and performed >80% by the 8th and final day of training. In the auditory cue-guided spatial task (Figure 1B), animals learned to go to one outer arm of a Y-shaped track when a sound was played, and to go to the other outer arm in the absence of sound. Similar to the W-track, correct performance meant that visits to the outer arms were interleaved with visits to the center arm. Animals performed above chance by the 4th day of training, and performed >75% by the 7th day of training.

Tetrodes were targeted to the prelimbic and infralimbic regions of medial prefrontal cortex (PFC) and to the dorsal CA1 region of the hippocampus (Figure 1C). A small fraction also targeted intermediate CA1 region in animals performing the W-track task (see Experimental Procedures; Figure S1). We recorded a total of 630 CA1 neurons and 353 PFC neurons in 6 animals over multiple days of behavior in the two tasks. We excluded a small number of fast-spiking, narrow-waveform cells, as well as cells with fewer than 50 spikes within SWR aligned windows (see Experimental Procedures), resulting in a total of 536 CA1 and 312 PFC putative excitatory neurons (see Table S1 for distribution of cells recorded across animals).

There are distinct patterns of hippocampal activity seen during exploration, when the theta rhythm is prominent, and during awake stillness, when memory replay during SWRs occurs (Buzsaki et al., 1983; Buzsaki, 1989). We therefore divided our data into two mutually exclusive sets of times based on movement speeds and power in the ripple band (150–250 Hz). Figure 2 illustrates these patterns of activity in an animal traversing a trajectory on a W-track. During the traversal, sequences of place cells representing locations are active and theta oscillations are visible (Figure 2A–C). When the animal stops to consume reward at the end of the trajectory, a dramatic shift in network state occurs, and SWR oscillations

(150–250 Hz) become prevalent (Figure 2A, 2D). As expected (Singer and Frank, 2009), SWRs occurred primarily at reward locations in both the behavioral tasks (Figure S2).

Overall, 35% (109/312) of PFC neurons were significantly SWR-modulated (see Table S2 for distribution of SWR-modulated cells across animals). Previous studies of PFC SWR activity during sleep reported that a large majority of modulated neurons were excited during sleep SWRs (Siapas and Wilson, 1998; Wierzynski et al., 2009). We were therefore surprised to see approximately equal numbers of excited and inhibited responses during awake SWRs (Figure 3A–3C; SWR-excited: 57/312, 18%; SWR-inhibited: 52/312 cells, 17%). Both populations showed transient responses to SWRs, with average firing rates returning to baseline values within ~300 ms of SWR onset. As similar proportions of SWR-excited and SWR-inhibited neurons were seen in the context of each of the two tasks (Figure 3C, Table S2), we combined data from the two tasks for the rest of the analyses, although analyses applied to the two tasks separately, and with exclusion of intermediate CA1 cells, yielded consistent results (not shown).

We then examined the timing of CA1 and PFC responses during SWRs. Overall, CA1 activity tended to precede PFC activity during SWRs, as in previous reports (Siapas and Wilson, 1998; Peyrache et al., 2009; Wierzynski et al., 2009). We computed the mean normalized SWR-aligned PSTHs for CA1 (n = 429), SWR-excited (n = 57), and SWR-inhibited (n = 52) PFC neuron populations (Figure 3D). The time of the peak CA1 population activity preceded both the peak of the SWR-excited and the trough of the SWR-inhibited PFC population activity (Figure 3D, 3E, mean ± sem time of peak for CA1, SWR-excited PFC and SWR-inhibited PFC cells = 54 ± 2 ms; 100 ± 9 ms; and 84 ± 10 ms, respectively; CA1 vs. PFC excited, $p< 10^{-11}$; CA1 vs. PFC inhibited, $p< 10^{-6}$; PFC excited vs. PFC inhibited, $p > 0.1$, rank-sum tests). Similarly, the time of SWR-modulation onset, measured as the time of firing rate increase/decrease to one standard deviation above/below the mean, was also significantly later for PFC than CA1 cells (Figure 3E *Right*, CA1 vs. PFC excited, $p< 10^{-9}$; CA1 vs. PFC inhibited, $p< 10^{-7}$; PFC excited vs. PFC inhibited, $p > 0.1$, rank-sum test). Finally, we also computed, for all SWR modulated CA1 and PFC neurons, the cross-covariance for all CA1-PFC pairs. We then separately averaged cross-covariances for pairs with an SWR-excited (n = 393 CA1-PFC pairs) or an SWR-inhibited PFC neuron (n = 320 CA1-PFC pairs). The peak (SWR-excited) or trough (SWR-inhibited) of the mean cross-covariance occurred at a time > 0 ms (Figure 3F; peak for excited cells: 13 ± 7 ms; trough for inhibited cells: 20 ± 7 ms).

SWR Modulation is Related to Theta Phase Locking of PFC Neurons

If SWR-related activity reflects the reactivation of specific PFC neurons that were coupled to the hippocampus during exploration, SWR-modulated PFC neurons would also tend to be modulated by the hippocampal theta rhythm. We first assessed theta phase locking by using a circular distribution to fit the theta-phase aligned PFC responses (Siapas et al., 2005) and used that fit to measure the circular concentration parameter (κ) (Experimental Procedures). Similar to previous reports (Jones and Wilson, 2005; Siapas et al., 2005), we found that 60% of PFC neurons (189 of 312, see Experimental Procedures) were significantly locked to theta. Also, as previously reported (Jones and Wilson, 2005; Siapas et al., 2005), CA1

neurons preferred the falling phase of theta while PFC neurons were most often phase-locked to the trough of theta (Figure 4A).

We next examined the relationship between SWR modulation and theta phase-locking in the PFC population. We found that the majority of significantly SWR-modulated neurons were also significantly phase-locked to hippocampal theta (Table S3). This included 44/57 SWR-excited neurons (77%) and 37/52 inhibited neurons (71%). There was no difference in the fraction of phase-locked cells in the excited and inhibited neuron populations ($p > 0.4$), but both had a higher fraction of phase locked cells than seen for SWR-unmodulated neurons (108/203 neurons: 53%; z-proportion tests between unmodulated and SWR excited: $p < 10^{-3}$; SWR inhibited: $p = 0.01$).

There was a parallel difference in the consistency of the theta phases at which different populations of PFC neurons tended to fire (Figure 4A). The circular concentration parameter (κ) for theta-modulated cells was larger in both the SWR-excited and SWR-inhibited populations, as compared to SWR-unmodulated neurons (Figure 4B, SWR-excited, SWR-inhibited and SWR-unmodulated $\kappa = 0.2 \pm 0.02$, 0.25 ± 0.04 and 0.12 ± 0.01 respectively; p's < 0.01 for SWR unmodulated vs. SWR-excited and SWR-inhibited; $p > 0.1$ for excited vs. inhibited; rank-sum tests). The converse analysis also showed that PFC neurons that were significantly theta modulated ($n = 189$) were also significantly more strongly SWR-modulated than neurons that were not theta modulated ($n = 123$) (Figure 4C, SWR modulation index: 5.2 ± 0.8 and 2.5 ± 0.4 respectively; $p < 0.01$, rank-sum test). Thus, SWR-modulation and theta phase-locking are related, suggesting a link between modulation during active movement and modulation during SWRs at the single-neuron level.

Finally, we also noted a difference in the uniformity of the distributions of theta-phase coupling across neuron types. SWR-excited neurons had a significantly narrower preferred phase distribution than both SWR-inhibited and SWR-unmodulated neurons (kuiper test for circular distribution, SWR-excited vs. SWR-inhibited, $n = 57$ vs. 52 neurons, $p > 0.1$; SWR-excited vs. SWR-unmodulated, $n = 57$ vs. 203 neurons, $p = 0.005$). In contrast, SWR-inhibited and SWR-unmodulated neurons did not differ in their concentration of preferred phases ($n = 52$ vs. 203 neurons, $p > 0.1$, kuiper test). Consistent with previous reports (Siapas et al., 2005; Sigurdsson et al., 2010), we also found that all PFC cells phase-locked optimally to hippocampal theta of the past (delay ~15 ms), as determined by systematically shifting the time of theta (data not shown).

SWR-Excited and Inhibited PFC Neurons Comprise Distinct Functional Populations

The differences in the theta modulation of SWR-excited, SWR-inhibited and SWR-unmodulated PFC cells suggest that SWR engagement could be a marker for functionally distinct populations. To further explore that possibility we asked if there were any differences in behavioral coding properties across populations (see Figure 5A for examples of spatial firing patterns). These analyses revealed clear distinctions between SWR-modulated and SWR–unmodulated cells, as well as distinctions between SWR-excited and SWR-inhibited cells.

We first compared mean firing rates during movement as a measure of overall engagement in the task. Interestingly, both SWR-excited and SWR-inhibited cells had significantly higher mean rates than SWR-unmodulated cells (Figure 5B; n = 57, 52 and 203 cells respectively for excited, inhibited and unmodulated cells; mean ± s.e.m. = 4.2 ± 0.5, 3.2 ± 0.4, 2.1 ± 0.2 Hz respectively; $p < 0.01$ for excited vs. unmodulated and $p < 10^{-4}$ inhibited vs. unmodulated, excited vs. inhibited $p > 0.1$, rank-sum test). SWR-excited, SWR-inhibited and SWR-unmodulated cells also differed in patterns of spatially-related firing. As previously reported (Baeg et al., 2003), PFC neurons as a whole were active across larger fractions of the environment than their CA1 counterparts, but SWR-excited neurons had significantly higher levels of coverage than both the SWR-inhibited and the SWR-unmodulated neurons (Figure 5C; coverages: excited: 0.70 ± 0.05; inhibited: 0.54 ± 0.05; unmodulated: 0.50 ± 0.02; $p < 0.01$ excited vs. inhibited, $p < 10^{-4}$ excited vs. unmodulated, $p > 0.1$ for inhibited vs. unmodulated; rank-sum test; see also Figure S3 for other measures of spatial activity).

SWR-excited and SWR-inhibited cells showed distinct patterns of movement speed preferences as well, with SWR excited cells showing a significantly higher firing rate-speed correlation than SWR inhibited cells (Figure 5D, 5E; $p < 0.01$ for excited vs. inhibited, rank-sum test). Further, the median of SWR-inhibited cells' speed correlations was significantly less than zero, indicating that these cells tended to fire most when animals were moving slowly (shuffle test, n = 1000, $p < 0.01$). In contrast, SWR-unmodulated cells showed a wider distribution of speed-spiking correlations that did not differ from the excited or inhibited populations (p's > 0.05). This suggests that SWR-inhibited cells were more active during periods of immobility when SWRs are prominent, as compared to high-speed movement. Indeed, we found that firing rates of SWR-inhibited cells just prior to SWRs were higher than those during high-speed movement. In contrast, SWR-excited cells showed the opposite pattern with a preference for movement times (Figure 5F, n = 57 vs. n = 52, rank-sum test, $p < 0.001$). Finally, we asked whether the cells differed in their tendency to reflect an important task event, the receipt of reward. PFC SWR-inhibited cells also showed a greater tendency to increase firing rates following reward than SWR-excited cells (Figure S3).

These differences also manifested as distinct patterns of co-firing within and between SWR-excited and SWR-inhibited PFC populations. We computed the cross-covariance between pairs of SWR-modulated neurons, restricted to movement times. We found a large and highly significant difference between the groups: SWR-excited cells tended to fire in close temporal proximity to other SWR-excited cells, SWR-inhibited cells tended to fire in proximity to other SWR-inhibited cells, but SWR-excited and SWR-inhibited cells tended not to fire together. This was evident both when we examined the population cross-covariance for pairs from each category (Figure 5G, *Left*) as well as the maximum zero lag cross covariance (Figure 5G, *Right*, n = 42 excited-excited pairs, n=36 inhibited-inhibited pairs, n = 73 excited-inhibited pairs, n = 369 unmodulated-unmodulated pairs; cross-covariance for excited-inhibited pairs was significantly lower than the other pair categories, p's< 0.001, rank-sum test). Taken together, these results indicate that SWR-excited and SWR-inhibited neurons form distinct functional ensembles that are engaged preferentially during movement and stillness, respectively.

Structured Reactivation of CA1-PFC Pairs during SWRs

These findings demonstrate that awake SWRs represent a prominent mode of hippocampal-prefrontal interaction where SWRs engage functionally distinct populations in PFC. Previous studies have shown that individual SWRs frequently contain replay events where specific sets of hippocampal neurons are active (Kudrimoti et al., 1999; Foster and Wilson, 2006; Diba and Buzsaki, 2007; Karlsson and Frank, 2009; Gupta et al., 2010; Pfeiffer and Foster, 2013). This is also apparent in correlated firing of CA1 neuron pairs, where pairs that are significantly correlated during theta oscillations in behavior also show enhanced correlations during SWR reactivation (O'Neill et al., 2008). If awake SWRs define a period where there is structured information flow between CA1 and PFC, we would expect that SWR-modulated PFC neurons would also be engaged differentially depending on which hippocampal neurons are active during each SWR.

As a first test of this hypothesis, we examined the structure of pairwise interactions between hippocampal and PFC neurons, using raw spike count correlations during SWRs. We measured the firing rates of hippocampal and SWR-modulated PFC neurons in a 0–200 ms window beginning at SWR onset, and then asked whether there were "SWR-correlated" CA1 and PFC pairs, defined as pairs of neurons where the CA1 firing rate across SWRs was significantly correlated with the associated PFC SWR firing rates.

We found that 16% of CA1-PFC neuron pairs were significantly SWR-correlated (n = 116 / 713 CA1-PFC pairs, $p < 0.05$ criterion for individual pairs; the 116 pairs comprised 94 unique SWR-modulated PFC cells and 53 unique CA1 cells). This was significantly more pairs than the ~5% we observed after shuffling the rates across SWRs ($p < 10^{-8}$, Z-test for proportions; see Experimental Procedures). There were similar proportions of significantly SWR-correlated pairs for both SWR-excited and SWR-inhibited PFC neurons (18%, n = 72/393 pairs for SWR-excited PFC neurons; 14%, 44/320 pairs for SWR-inhibited PFC neurons; histograms in Figure S4). Interestingly, these included both positive and negative correlations with both SWR-excited and SWR-inhibited PFC populations (Figure 6A, 6B *Top*). Thus, spiking activity of neuronal pairs across CA1 and PFC during SWRs is often strongly correlated.

If these patterns of positive and negative correlations reflect the reactivation of behaviorally related spiking patterns, we would expect that CA1–PFC pairs that fired together during theta periods (corresponding to active behavior) would show positive SWR correlations, while pairs that did not would show negative correlations. We therefore calculated theta-period correlations between CA1-PFC neuron pairs as the peak of the standardized Z-scored cross-covariance during movement (Figure 6A, 6B *Bottom*) (Siapas et al., 2005).

This analysis revealed a significant relationship between theta cross-covariance and SWR-correlations ($r = 0.39$, n = 713 pairs, $p < 10^{-4}$, regression test), for both the SWR-excited and SWR-inhibited populations (Figure 6C; SWR-excited neurons: $r = 0.39$, n = 393 pairs, $p < 10^{-4}$; SWR-inhibited neurons: $r = 0.39$, n = 320 pairs, $p < 10^{-4}$, regression test). The SWR-excited and SWR-inhibited populations showed a similar degree of correlation (shuffle test, n = 1000, $p > 0.1$). The identification of CA1-PFC pairs with strong SWR and theta correlations also allowed us to ask whether CA1 spiking tended to lead PFC spiking during

behavior as it did during SWRs. We examined the subset of CA1-PFC pairs with significant and positive SWR correlations, which also tended to have high theta cross-covariances, and found that the peaks of these cross-covariances reflected an overall tendency for CA1 to lead PFC (Figure S4).

We next examined whether these results could be extended beyond pairwise interactions. We used a generalized linear model (GLM) with a log link function to predict SWR-related spiking of single PFC neurons from the activity of the simultaneously recorded CA1 ensembles. The GLM model confirmed the presence of functional links between CA1 and PFC ensembles (Figure 6D). Interestingly, the same CA1 neuron could be positively predictive of the spiking of one PFC neuron and negatively predictive of the activity of another. Conversely, a PFC neuron could be positively predicted by one CA1 neuron and negatively predicted by a different CA1 neuron. These findings demonstrate highly specific patterns of interaction across structures.

Using cross validation to ensure that our models did not over fit the data, we found that that prediction performance was better than chance for SWR-modulated PFC cells (n = 77) and increased with the size of the CA1 ensemble (Figure 6E, striped bars; n = 30, 20, 27 PFC cells, 1-way ANOVA, main effect of cell count group: $p < 10^{-4}$). PFC SWR-modulated cells were better predicted than SWR-unmodulated cells but predictions of SWR-excited and SWR-inhibited cells did not differ from one another (2-way ANOVA, modulated n = 77 vs. unmodulated n = 102: $p < 10^{-4}$; SWR-excited n = 40; SWR-inhibited n = 37: p = 0.29; main effect of cell count groups: p's$< 10^{-7}$). Lastly, since we found that pairwise CA1-PFC correlations during behavior were related to SWR firing rate correlations, we asked whether the spiking of PFC neurons during SWRs could be predicted using a model constructed on activity during movement rather than during SWRs (Figure 6E, white bars). We found that theta-derived models could in many cases predict PFC SWR-firing and the accuracy of this prediction also increased with the size of the CA1 ensemble. This prediction was significantly better for SWR-modulated cells than unmodulated cells (2-way ANOVA, SWR-modulated vs. unmodulated, p = 0.02, cell count group, $p < 10^{-7}$). It is important to note, however, that this analysis does not demonstrate a causal directionality from movement-related experience to SWRs. Indeed, using SWR-derived models to predict theta activity also yielded above-chance predictions, although the quality of these predictions was significantly lower than using theta-trained models to predict SWR activity (2-way ANOVA: model type X cell count interaction: $p < 0.01$). Finally, as expected, reversing the direction of prediction also revealed that PFC activity could significantly predict SWR-associated CA1 spiking (Figure S4). Overall, these findings demonstrate that there is close coordination between CA1 and PFC activity during SWRs that is similar to activity patterns seen during movement.

Reactivation in the CA1-PFC Network Reflects Spatially Related Ensembles

The reactivation of CA1-PFC pairs during SWRs, consisting of both positive and negative correlations, is similar to that reported previously between CA1 neuronal pairs during sleep (O'Neill et al., 2008). In that case, the pattern of CA1 pair correlations was related to the spatial overlap of the neurons' place fields. We therefore asked if the same was true for

CA1-PFC correlations, and looked at the relationship between spatial firing patterns of CA1 and PFC neuron pairs. While PFC neurons tend to be active across wide swaths of the environment, they nevertheless show some degree of selectivity across different trajectories (Baeg et al., 2003; Hyman et al., 2005; Jones and Wilson, 2005) (Figure 5), likely as a result of task-related firing patterns that develop with experience (Jung et al., 1998; Baeg et al., 2003).

We found that the similarity between the spatial response profiles of the CA1 and PFC neurons, quantified as a spatial correlation, was related to their SWR correlation for both SWR-inhibited and SWR-excited neurons (See example in Figure 7A, 7B; population results in Figure 7C; SWR-excited neurons: $r = 0.2$, $n = 393$ pairs, $p < 10^{-3}$; SWR-inhibited neurons: $r = 0.36$, $n = 320$ pairs, $p < 10^{-4}$, regression test). Across the population, SWR-correlated pairs had significantly higher spatial correlations than SWR-uncorrelated pairs, and SWR-anticorrelated pairs had negative and significantly lower spatial correlations than SWR-uncorrelated pairs (SWR-excited: $n = 72$ pairs, SWR-inhibited $n = 44$ pairs, p's $< 10^{-4}$, rank-sum tests). Interestingly, the relationship between spatial correlation and SWR correlation was significantly stronger for SWR-inhibited neurons than SWR-excited neurons (shuffle test, $n = 1000$, $p < 0.01$). This higher correlation was likely the result of the higher spatial specificity of SWR-inhibited neurons as compared to SWR-excited neurons: when we subsampled to choose SWR-excited and inhibited neurons with matched spatial selectivity, both groups showed a similarly strong relationship between spatial and SWR-correlations (Figure S5). Finally, we also examined the content of hippocampal replay events as it related to PFC spiking. Here we were limited by the small number of datasets in which both sufficient CA1 ensembles and a sufficient number of SWR-modulated PFC cells were identified. Nonetheless, analysis of this small set of replay events revealed patterns of joint activity consistent with coordinated replay across structures (Figure S6).

Task Related CA1-PFC Correlations are Not Present in Preceding Rest Periods

These findings indicate that there is structured activity across hippocampus and PFC during behavior and during awake SWRs, and raise the question of whether this is the result of behavioral experience or simply a reflection of pre-existing connections. We therefore compared CA1-PFC behavioral correlations seen during the behavioral task to those in pre-task periods in a rest box (*pre-rest* sessions). We focused on data from the W-track task to exclude sessions where sound was played during rest in the Y-track task, although the results were the same when we combined data from both tracks (Figure S7).

Comparing the SWR response correlations between CA1-PFC pairs revealed that there was no detectable relationship between awake SWR correlations and SWR correlations in pre-rest periods (Figure 8A). Thus, the structure of SWR correlations is specific to the behavioral experience. Similarly, we saw no relationship between pre-task SWR correlations and either movement-related correlations (Figure 8B) or spatial correlations (Figure 8C). Moreover, GLMs trained on SWR activity in the awake state (CA1 ensemble activity predicting PFC spiking) were unable to predict PFC spiking in SWRs during pre-rest periods (shuffle test, $n = 1000$, $p > 0.5$), and performed significantly worse than prediction of PFC spiking in SWRs during behavior (Figure 8D). These results indicate that the observed CA1-

PFC coordination during awake SWRs is specific to task performance and is not detectable before each day's experience.

DISCUSSION

Our results establish awake SWRs as a prominent network activity pattern mediating hippocampal-PFC interactions during behavior. We found coherent reactivation of behaviorally concordant information across hippocampal-PFC networks during awake SWRs. We also show that this reactivation includes not only the expected excitation of some PFC cells, but also inhibition of other PFC cells. Moreover, these SWR-excited and SWR-inhibited populations had distinct spatial and temporal firing properties, where SWR-excited cells were more active during movement while SWR-inhibited cells were more active around the times of SWRs during stillness and following reward. Finally, we found that the coordinated firing was specific to the task epoch, and was not detectable in the preceding rest period.

Awake SWRs are of particular interest because they have been causally linked to memory: interrupting awake SWRs is sufficient to impair learning and performance in a situation where animals needed to link multiple experiences across time and make decisions based on those experiences (Jadhav et al., 2012). Examination of hippocampal activity during awake SWRs has revealed that these events can contain sequential spiking that recapitulates patterns seen during both recent (Foster and Wilson, 2006; Diba and Buzsaki, 2007; Davidson et al., 2009) and more remote past experiences (Karlsson and Frank, 2009; Gupta et al., 2010). Further, the intensity of hippocampal reactivation during awake SWRs can be predictive of whether an upcoming decision will be correct or incorrect (Singer et al., 2013), and the content of awake replay events can be predictive of upcoming choices in certain task contexts (Pfeiffer and Foster, 2013). While the specific role that SWR activity plays in memory retrieval and decision-making processes remains unclear, one possibility is that it contributes to deliberation by transmitting sequences corresponding to either specific past experiences (Carr et al., 2011) or possible future options to other brain areas (Yu and Frank, 2015). The PFC is known to play a central role in these retrieval and decision-making processes (Hasegawa, 2000; Miller and Cohen, 2001; Sakai, 2003; Wiltgen et al., 2004; Jung et al., 2008; Tse et al., 2011).

Our findings provide support for the possibility that awake SWR-related activity in the PFC supports computations related to the specific content of the corresponding SWR-related hippocampal activity (Yu and Frank, 2015). We found that the spiking activity of a substantial fraction of PFC neurons is modulated during awake hippocampal SWRs. Further, correlations between CA1-PFC pairs during awake SWRs reflected pairwise correlations during active exploration, measured by the theta-period correlation structure as well as correlation of spatial receptive fields. Neuron pairs in the CA1-PFC network that were more correlated during reactivation tended to represent overlapping spatial locations, whereas those that were anti-correlated or uncorrelated during reactivation represented non-overlapping locations. At the population level, we found specific patterns of simultaneous positive and negative correlations, implying that specific groups of CA1 and PFC neurons are co-active during SWRs. These patterns reflect structure seen in the theta state, since a

GLM model built using theta-associated spiking patterns was able to significantly predict activity during SWRs. Further, spiking from either CA1 or PFC could be used to predict activity in the other, indicating the presence of coherent functional ensembles across the two regions. Therefore, our findings imply very precise coordinated activity in the CA1-PFC network during SWRs, which is well suited to support memory processes.

We also found a bias towards CA1 leading PFC directionality during both SWRs and theta, as in previous studies (Siapas and Wilson, 1998; Peyrache et al., 2009; Wierzynski et al., 2009)(Jones and Wilson, 2005; Siapas et al., 2005; Sigurdsson et al., 2010). This bias is consistent with recent reports that ventral hippocampal CA1 inputs to PFC are important for spatial representations and information encoding in a working memory task (Spellman et al., 2015). At the same time, there is clear evidence of PFC influence on CA1 during behavior in the context of coding for past and future location (Ito et al., 2015), indicating bidirectional information flow between these structures during behavior. Importantly, this information flow does not imply monosynaptic connectivity. In our case, a large majority of our hippocampal recordings were in dorsal CA1 (~ 88%), which has only an anatomically minor projection to PFC (Cenquizca and Swanson, 2007). Instead, the observed coordinated reactivation likely depend on indirect connectivity and/or the interconnectivity between dorsal areas of the hippocampus and intermediate and ventral hippocampus (Witter and Amaral, 2004), from which strong direct projections to PFC arise (Cenquizca and Swanson, 2007).

Surprisingly, we also found that PFC reactivation involves cell-specific excitation and inhibition. This observation is consistent with a recent report showing excitatory and inhibitory responses of neurons in the VTA during hippocampal SWRs (Gomperts et al., 2015), and taken together these findings suggest the possibility of widespread activation and inhibition of neurons outside the hippocampus during SWRs. While we and others have hypothesized that awake SWR-related activity could drive the activity of specific populations of neurons in the context of memory retrieval, memory consolidation and decision-making (O'Neill et al., 2010; Carr et al., 2011; Yu and Frank, 2015), the possibility of structured inhibition of PFC activity has not, to our knowledge, been proposed. Moreover, we found that SWR-excited and SWR-inhibited PFC populations comprised of functionally distinct groups: SWR-excited cells had more spatially diffuse firing and tended to be active at higher movement speeds, while SWR-inhibited cells had more spatially concentrated firing and tended to be active at the lower movement speeds where SWRs are more common (O'Neill et al., 2006; Cheng and Frank, 2008; Karlsson and Frank, 2009; Carr et al., 2011). SWR-inhibited cells were also more selective for reward. Further, cell pairs with one SWR-excited and one SWR-inhibited PFC neuron were rarely coactive in a one second window, while pairs comprising like-modulated cells were often strongly coactive during movement.

The content-specific inhibition of many PFC cells during SWRs suggest that upon the initiation of an SWR, the representation in PFC related to the current state can be suppressed and replaced with a representation of recent active behavior consistent with the representation reactivated in CA1. SWR-inhibited PFC cells are most strongly suppressed when the spatial content of a hippocampal reactivation event is inconsistent with the movement-related activity of the PFC cell. In contrast, when the spatial content of the

reactivation is behaviorally consistent, the inhibition is reduced, indicating that the cell could continue to signal strongly to downstream neurons. Thus, SWR-related inhibition of PFC is well suited to suppress ongoing PFC activity that is inconsistent with the content of the replayed information coming from the hippocampus.

Finally, our results also complement previous studies of hippocampal and cortical reactivation during sleep. Sleep SWRs have been linked to memory consolidation (Born and Wilhelm, 2012) and reactivation during SWRs has been shown to occur within PFC during sleep (Peyrache et al., 2009), but whether this reactivation reflects the specific content of simultaneous hippocampal reactivation events has not been examined. Similarly, reports of 'reverberation' of prior activity across multiple structures during offline periods after behavior (Hoffman and McNaughton, 2002; Ribeiro et al., 2004) did not examine activity in the hippocampus. That said, in one study that looked for episodes of concurrent reactivation between hippocampus and visual cortex during slow wave sleep, a small number of coherent reactivation events were seen (Ji and Wilson, 2007). Our results show that during awake SWRs, coherent reactivation is common, and that it engages both excitation and inhibition in the PFC. This establishes SWRs as a network state that is well suited to support awake memory processes, complementing the role of sleep SWRs in memory consolidation.

EXPERIMENTAL PROCEDURES

An overview of experimental procedures is presented below. See Supplemental Experimental Procedures for more details.

Animals and Experimental Overview

Six male Long Evans rats weighing 450–550 grams were used in this study. All procedures were approved by the Institutional Animal Care and Use Committee at the University of California, San Francisco and conformed to National Institutes of Health guidelines. (Jadhav et al., 2012). Animals were pre-trained to seek liquid food rewards on a raised linear track (Jadhav et al., 2012). Following the conclusion of the experiments, we made micro-lesions through each electrode tip to mark recording locations

Behavioral Tasks

Rats (n = 3 per task) learned either a W-track or a Y-track auditory cue-guided spatial task across 8–12 days, in multiple run sessions per day with interleaving rest sessions. Data were pooled across all sessions within a day. For the W-track task (2 sessions per day), rats were rewarded upon returning to the center well after visits to either side well, and starting from the center well, when the opposite side well from the previous side trajectory was chosen. In the Y-track auditory-cue guided spatial task, following a reward in the home well, in ~75% of trials the rat were rewarded upon arriving at the end of the "silent arm". In a pseudo-random ~25% of trials, 5 seconds after poking in the home well, a specific sound was emitted from a speaker, in which case rats were rewarded in the "sound arm".

Surgical Implantation and Electrophysiology

Surgical implantation procedures were as previously described (Jadhav et al., 2012). Animals were implanted with a microdrive array with 21 independently moveable tetrodes at the following coordinates: W-track: right dorsal hippocampal region CA1 (−3.6 mm AP and 2.2 mm ML), right PFC (+3.0 mm AP and 0.7 mm ML, 5 degree angle in one animal), and intermediate CA1 (−6.3 mm AP and 5.5 mm ML, in two animals); Y-track task: left dorsal CA1 (−3.6 mm AP and −2.2 mm ML), left PFC (+3.0 mm AP and −1 mm ML); left primary auditory cortex (−4.8mm AP and −5.5 mm ML, 25 degrees laterally from midline). Figure S1 shows the recording locations for all electrodes in all animals, and distribution of cells across animals is shown in Table S1. Only data from hippocampal and prefrontal recordings are reported here.

Data were collected using the NSpike data acquisition system (Karlsson and Frank, 2009; Jadhav et al., 2012) (L.M.F. and J. MacArthur, Harvard Instrumentation Design Laboratory). We recorded continuous local field potentials (LFP, filtered 0.5–400 Hz and sampled at 1.5 kHz) from all tetrodes. Spike data were sampled at 30 kHz, digitally filtered between 300 or 600 Hz and 6 kHz and threshold crossing events were saved to disk (40 samples at 30 kHz). An infrared light emitting diode array with a large and a small cluster of diodes was attached to the preamps during recording. Behavior sessions were recorded with an overhead monochrome CCD camera (30 fps) and the animal's position and speed were detected online using the infrared diodes.

Data Analysis

Data analysis was performed using custom routines in Matlab (MathWorks, Natick, MA). We used non-parametric tests for statistical comparisons throughout the manuscript unless otherwise noted. All values reported are mean ± sem unless otherwise noted.

SWR Detection and Modulation

SWRs were detected using LFPs filtered in the 150–250 Hz range on multiple CA1 tetrodes as previously described (Karlsson and Frank, 2009). We limited our analysis to putative PFC and CA1 excitatory neurons with sufficient number of spikes. We developed an SWR-modulation metric (see Supplemental Experimental Procedures) which was based on comparing the response in the 0–200 ms window after SWR onset to shuffled data. PFC SWR-modulated neurons were categorized as SWR-excited or SWR-inhibited by comparing the rate in the 0–200 ms window after SWR onset with the rate in a pre-SWR background window −500 to −100 ms window before SWR onset. Timing and cross-covariance of the SWR-response was calculated using the SWR-aligned rasters.

Theta Phase Locking

Theta phase-locking was calculated using the methods developed in previous reports (Siapas et al., 2005). Theta oscillations were filtered in the 6–12 Hz range in the LFP down-sampled to 150 Hz. We used a CA1 tetrode located in corpus callosum to measure theta phase (Lubenov and Siapas, 2009). Theta periods were assigned based on a speed criterion of >5 cm/sec and no SWRs detected on any of the CA1 tetrodes with a 3 s.d. criterion.

Spatial Properties

Spatial firing properties of neurons were computed using occupancy-normalized linearized firing rates of neurons (Figure 5, S3, 7). Spatial coverage of neurons was defined as the fraction of area above 25% of the peak firing rate of the neuron across all 4 trajectories got neurons with a peak spatial firing rate > 3 Hz. Spatial correlations between neurons were also calculated using the linearized firing rates.

SWR Correlations and Theta Cross-covariance

SWR correlations between pairs of CA1-PFC neurons were measured as the correlation coefficient between the magnitudes of the spiking responses of the two neurons in the 0–200 ms aligned to SWR onset. Standardized cross-covariance during theta (Figure 5 and 6) was calculated as in previous reports (Siapas et al., 2005). Only theta periods that were at-least 1 second long were included in the analysis.

GLM

For each SWR modulated PFC neuron, we trained a generalized linear model (GLM) with a log link function to predict SWR-related spiking of that PFC neuron from the activity of the simultaneously recorded CA1 ensemble. To determine predictive significance, we used a cross-validation approach, training on 90% of the SWR-responses and predicting the remainder.

Supplementary Material

Refer to Web version on PubMed Central for supplementary material.

Acknowledgments

This work was supported by NIH Grants R00 MH100284 and a Sloan research fellowship (S.P.J.), RO1 MH090188 (L.M.F.), and EMBO and ELSC postdoctoral fellowships (G.R.). We thank Irene Grossrubatscher for assistance with histology, Ryan Young for assistance with analysis, and Brett Mensh for feedback on the manuscript.

References

Amaral, DG.; Witter, MP. Hippocampal Formation. In: Paxinos, C., editor. The Rat Nervous System. Academic Press; 1995. p. 443-493.

Baeg EH, Kim YB, Huh K, Mook-Jung I, Kim HT, Jung MW. Dynamics of population code for working memory in the prefrontal cortex. Neuron. 2003; 40:177–188. [PubMed: 14527442]

Benchenane K, Peyrache A, Khamassi M, Tierney PL, Gioanni Y, Battaglia FP, Wiener SI. Coherent theta oscillations and reorganization of spike timing in the hippocampal-prefrontal network upon learning. Neuron. 2010; 66:921–936. [PubMed: 20620877]

Born J, Wilhelm I. System consolidation of memory during sleep. Psychological research. 2012; 76:192–203. [PubMed: 21541757]

Buzsaki G. Two-stage model of memory trace formation: a role for “noisy” brain states. Neuroscience. 1989; 31:551–570. [PubMed: 2687720]

Buzsaki G. Hippocampal sharp wave-ripple: A cognitive biomarker for episodic memory and planning. Hippocampus. 2015

Buzsaki G, Leung LW, Vanderwolf CH. Cellular bases of hippocampal EEG in the behaving rat. Brain Res. 1983; 287:139–171. [PubMed: 6357356]

Carr MF, Jadhav SP, Frank LM. Hippocampal replay in the awake state: a potential substrate for memory consolidation and retrieval. Nat Neurosci. 2011; 14:147–153. [PubMed: 21270783]

Cenquizca LA, Swanson LW. Spatial organization of direct hippocampal field CA1 axonal projections to the rest of the cerebral cortex. Brain Res Rev. 2007; 56:1–26. [PubMed: 17559940]

Cheng S, Frank LM. New experiences enhance coordinated neural activity in the hippocampus. Neuron. 2008; 57:303–313. [PubMed: 18215626]

Davidson TJ, Kloosterman F, Wilson MA. Hippocampal replay of extended experience. Neuron. 2009; 63:497–507. [PubMed: 19709631]

Diba K, Buzsaki G. Forward and reverse hippocampal place-cell sequences during ripples. Nat Neurosci. 2007; 10:1241–1242. [PubMed: 17828259]

Dragoi G, Buzsaki G. Temporal encoding of place sequences by hippocampal cell assemblies. Neuron. 2006; 50:145–157. [PubMed: 16600862]

Dudai Y. The neurobiology of consolidations, or, how stable is the engram? Annu Rev Psychol. 2004; 55:51–86. [PubMed: 14744210]

Eichenbaum, H.; Cohen, NJ. From Conditioning to Conscious Recollection. New York: Oxford University Press; 2001.

Euston DR, Gruber AJ, McNaughton BL. The role of medial prefrontal cortex in memory and decision making. Neuron. 2012; 76:1057–1070. [PubMed: 23259943]

Euston DR, Tatsuno M, McNaughton BL. Fast-forward playback of recent memory sequences in prefrontal cortex during sleep. Science. 2007; 318:1147–1150. [PubMed: 18006749]

Floresco SB, Seamans JK, Phillips AG. Selective roles for hippocampal, prefrontal cortical, and ventral striatal circuits in radial-arm maze tasks with or without a delay. J Neurosci. 1997; 17:1880–1890. [PubMed: 9030646]

Foster DJ, Wilson MA. Reverse replay of behavioural sequences in hippocampal place cells during the awake state. Nature. 2006; 440:680–683. [PubMed: 16474382]

Gomperts SN, Kloosterman F, Wilson MA. VTA neurons coordinate with the hippocampal reactivation of spatial experience. eLife. 2015; 4

Gordon JA. Oscillations and hippocampal-prefrontal synchrony. Curr Opin Neurobiol. 2011; 21:486–491. [PubMed: 21470846]

Gupta AS, van der Meer MA, Touretzky DS, Redish AD. Hippocampal replay is not a simple function of experience. Neuron. 2010; 65:695–705. [PubMed: 20223204]

Hasegawa I. Neural mechanisms of memory retrieval: role of the prefrontal cortex. Rev Neurosci. 2000; 11:113–125. [PubMed: 10718149]

Hoffman KL, McNaughton BL. Coordinated reactivation of distributed memory traces in primate neocortex. Science. 2002; 297:2070–2073. [PubMed: 12242447]

Hyman JM, Zilli EA, Paley AM, Hasselmo ME. Medial prefrontal cortex cells show dynamic modulation with the hippocampal theta rhythm dependent on behavior. Hippocampus. 2005; 15:739–749. [PubMed: 16015622]

Ito HT, Zhang SJ, Witter MP, Moser EI, Moser MB. A prefrontal-thalamo-hippocampal circuit for goal-directed spatial navigation. Nature. 2015; 522:50–55. [PubMed: 26017312]

Jadhav SP, Kemere C, German PW, Frank LM. Awake hippocampal sharp-wave ripples support spatial memory. Science. 2012; 336:1454–1458. [PubMed: 22555434]

Ji D, Wilson MA. Coordinated memory replay in the visual cortex and hippocampus during sleep. Nat Neurosci. 2007; 10:100–107. [PubMed: 17173043]

Jones MW, Wilson MA. Theta rhythms coordinate hippocampal-prefrontal interactions in a spatial memory task. PLoS Biol. 2005; 3:e402. [PubMed: 16279838]

Jung MW, Baeg EH, Kim MJ, Kim YB, Kim JJ. Plasticity and memory in the prefrontal cortex. Rev Neurosci. 2008; 19:29–46. [PubMed: 18561819]

Jung MW, Qin Y, McNaughton BL, Barnes CA. Firing characteristics of deep layer neurons in prefrontal cortex in rats performing spatial working memory tasks. Cereb Cortex. 1998; 8:437–450. [PubMed: 9722087]

Karlsson MP, Frank LM. Awake replay of remote experiences in the hippocampus. Nat Neurosci. 2009; 12:913–918. [PubMed: 19525943]

Kudrimoti HS, Barnes CA, McNaughton BL. Reactivation of hippocampal cell assemblies: effects of behavioral state, experience, and EEG dynamics. Journal of Neuroscience. 1999; 19:4090–4101. [PubMed: 10234037]

Lubenov EV, Siapas AG. Hippocampal theta oscillations are travelling waves. Nature. 2009; 459:534–539. [PubMed: 19489117]

Miller EK, Cohen JD. An integrative theory of prefrontal cortex function. Annu Rev Neurosci. 2001; 24:167–202. [PubMed: 11283309]

O'Neill J, Pleydell-Bouverie B, Dupret D, Csicsvari J. Play it again: reactivation of waking experience and memory. Trends Neurosci. 2010; 33:220–229. [PubMed: 20207025]

O'Neill J, Senior T, Csicsvari J. Place-selective firing of CA1 pyramidal cells during sharp wave/ripple network patterns in exploratory behavior. Neuron. 2006; 49:143–155. [PubMed: 16387646]

O'Neill J, Senior TJ, Allen K, Huxter JR, Csicsvari J. Reactivation of experience-dependent cell assembly patterns in the hippocampus. Nat Neurosci. 2008; 11:209–215. [PubMed: 18193040]

Peyrache A, Khamassi M, Benchenane K, Wiener SI, Battaglia FP. Replay of rule-learning related neural patterns in the prefrontal cortex during sleep. Nat Neurosci. 2009; 12:919–926. [PubMed: 19483687]

Pfeiffer BE, Foster DJ. Hippocampal place-cell sequences depict future paths to remembered goals. Nature. 2013; 497:74–79. [PubMed: 23594744]

Ribeiro S, Gervasoni D, Soares ES, Zhou Y, Lin SC, Pantoja J, Lavine M, Nicolelis MA. Long-lasting novelty-induced neuronal reverberation during slow-wave sleep in multiple forebrain areas. PLoS Biol. 2004; 2:E24. [PubMed: 14737198]

Sakai K. Reactivation of memory: role of medial temporal lobe and prefrontal cortex. Rev Neurosci. 2003; 14:241–252. [PubMed: 14513867]

Siapas AG, Lubenov EV, Wilson MA. Prefrontal phase locking to hippocampal theta oscillations. Neuron. 2005; 46:141–151. [PubMed: 15820700]

Siapas AG, Wilson MA. Coordinated interactions between hippocampal ripples and cortical spindles during slow-wave sleep. Neuron. 1998; 21:1123–1128. [PubMed: 9856467]

Sigurdsson T, Stark KL, Karayiorgou M, Gogos JA, Gordon JA. Impaired hippocampal-prefrontal synchrony in a genetic mouse model of schizophrenia. Nature. 2010; 464:763–767. [PubMed: 20360742]

Singer AC, Carr MF, Karlsson MP, Frank LM. Hippocampal SWR Activity Predicts Correct Decisions during the Initial Learning of an Alternation Task. Neuron. 2013; 77:1163–1173. [PubMed: 23522050]

Singer AC, Frank LM. Rewarded outcomes enhance reactivation of experience in the hippocampus. Neuron. 2009; 64:910–921. [PubMed: 20064396]

Skaggs WE, McNaughton BL, Wilson MA, Barnes CA. Theta phase precession in hippocampal neuronal populations and the compression of temporal sequences. Hippocampus. 1996; 6:149–172. [PubMed: 8797016]

Spellman T, Rigotti M, Ahmari SE, Fusi S, Gogos JA, Gordon JA. Hippocampal-prefrontal input supports spatial encoding in working memory. Nature. 2015; 522:309–314. [PubMed: 26053122]

Squire LR. Memory and the hippocampus: a synthesis from findings with rats, monkeys, and humans [published erratum appears in Psychol Rev 1992 Jul;99(3):582]. Psychol Rev. 1992; 99:195–231. [PubMed: 1594723]

Tse D, Takeuchi T, Kakeyama M, Kajii Y, Okuno H, Tohyama C, Bito H, Morris RG. Schema-dependent gene activation and memory encoding in neocortex. Science. 2011; 333:891–895. [PubMed: 21737703]

Wang GW, Cai JX. Disconnection of the hippocampal-prefrontal cortical circuits impairs spatial working memory performance in rats. Behav Brain Res. 2006; 175:329–336. [PubMed: 17045348]

Wang GW, Cai JX. Reversible disconnection of the hippocampal-prelimbic cortical circuit impairs spatial learning but not passive avoidance learning in rats. Neurobiol Learn Mem. 2008; 90:365–373. [PubMed: 18614383]

Wierzynski CM, Lubenov EV, Gu M, Siapas AG. State-dependent spike-timing relationships between hippocampal and prefrontal circuits during sleep. Neuron. 2009; 61:587–596. [PubMed: 19249278]

Wiltgen BJ, Brown RA, Talton LE, Silva AJ. New circuits for old memories: the role of the neocortex in consolidation. Neuron. 2004; 44:101–108. [PubMed: 15450163]

Witter, MP.; Amaral, DG. Hippocampal formation. In: Paxinos, G., editor. The rat nervous system. San Diego, CA: Elsevier Academic Press; 2004. p. 635-704.

Yu JY, Frank LM. Hippocampal-cortical interaction in decision making. Neurobiol Learn Mem. 2015; 117C:34–41. [PubMed: 24530374]

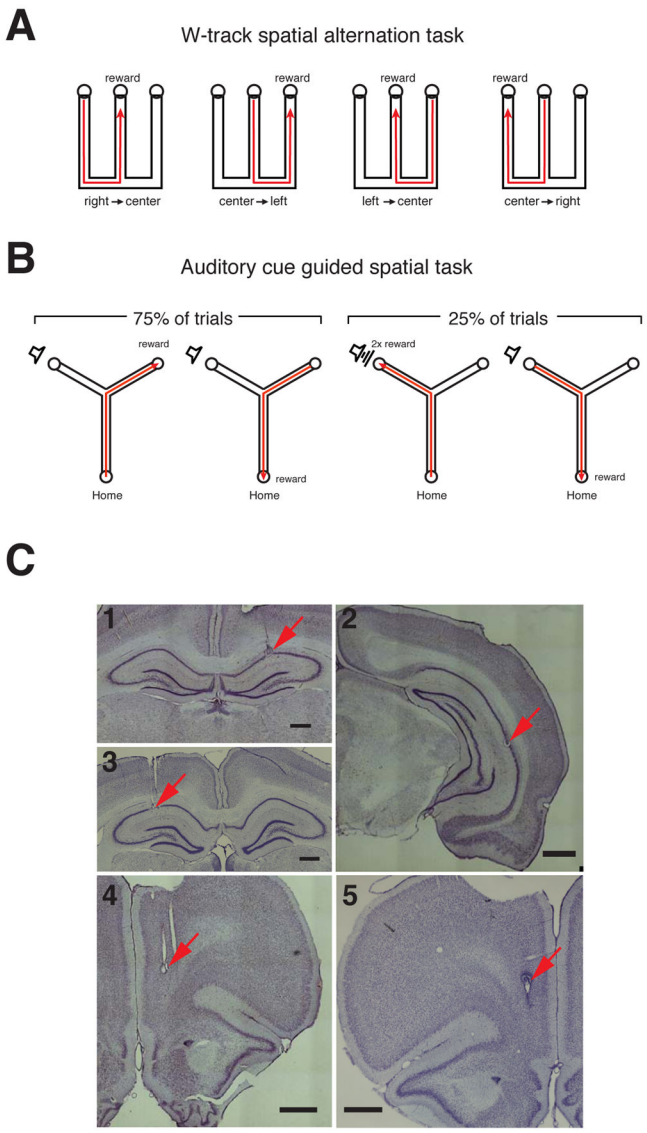

Figure 1. Behavior Paradigms and Recording Locations

(A) W-track. Animals had to learn to alternate between the three arms of the W-track for reward.

(B) Y-track. In each trial initiated by poking in the home well, animals had to learn to visit the "silent well" when no sound was presented (75% of trials) and the "sound well" when the target sound was presented (25% of trials).

(C) Histology illustrating recording locations. Nissl stained coronal sections showing electrode tracks and lesion location. (C1) W-track: dorsal CA1, (C2) W-track: intermediate CA1, (C3) Y track: dorsal CA1, (C4) W-track: medial PFC, (C5) Y track medial PFC. Scale bars are 1 mm.

See also Figure S1 and Table S1.

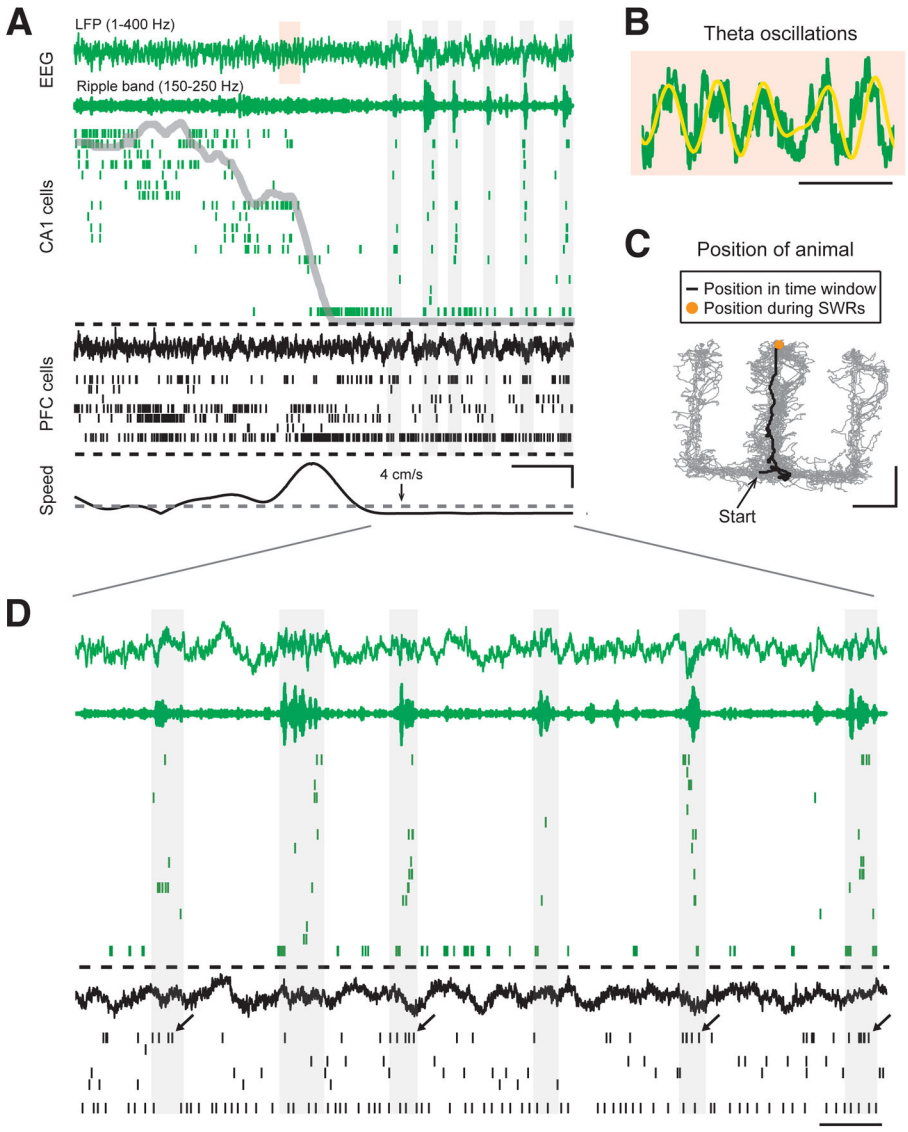

Figure 2. Two Distinct Network Activity Patterns in the Hippocampus During Behavior

(A) Spike and local field potential (LFP) activity in CA1 region of the hippocampus (green) and PFC (black) as an animal approaches a reward well in the W-track spatial alternation task. From top to bottom, the plot shows respectively: broadband LFP (1–400 Hz) in CA1, ripple band filtered LFP (150–250 Hz) in CA1, raster plot with spikes from 18 CA1 place cells, broadband LFP in PFC, raster plot with spikes from 7 PFC neurons, and animal speed. Linear distance of the animal from the reward well is overlaid on the CA1 raster (grey line). The threshold speed, 4 cm/s, used to detect SWRs is indicated on the speed plot. Vertical gray rectangle backgrounds denote SWRs detected in CA1 LFP. Scale bars are 2 sec (horizontal), and 10 cm/s (vertical). **(B)** Shaded area over CA1 LFP from (A) on an expanded time scale. Theta filtered LFP (6–12 Hz) is shown overlaid with the broadband LFP. Scale bar = 250 ms.

(C) Position of the animal on the W-track as it approaches the center reward well and stops to consume reward. Scale bar = 20 cm.

(D) Time period marked by lines from (A) shown on an expanded time scale, illustrating activity in CA1 and PFC when the animal is stationary at the reward well. Note that one of the PFC neurons shows increased spiking during a subset of the hippocampal SWRs (marked by arrows). Scale bar = 500 ms.

See also Figure S2.

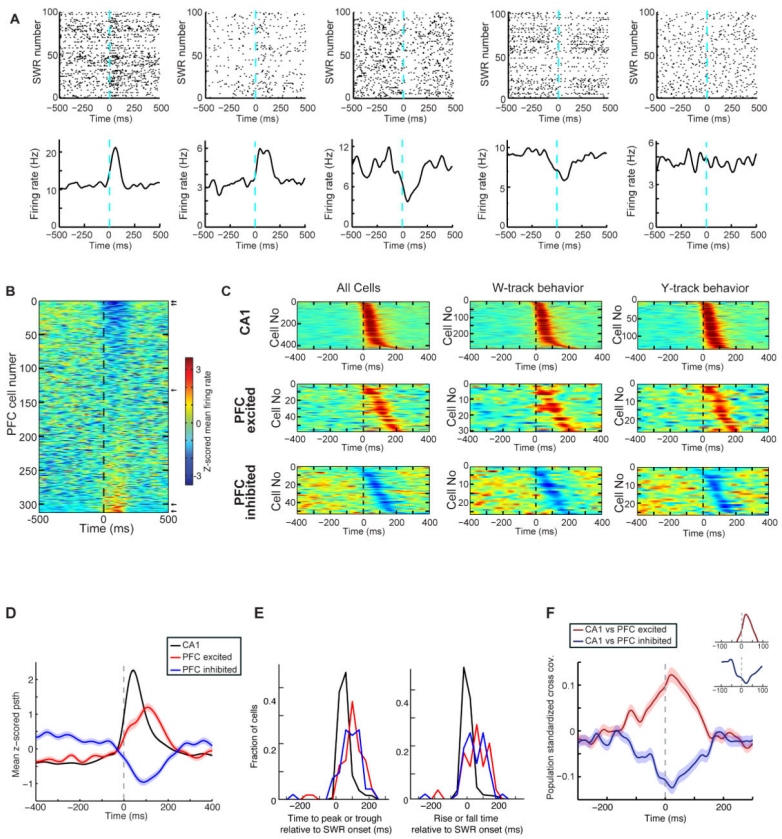

Figure 3. Modulation of PFC Neuronal Spiking During Awake Hippocampal SWRs

(A) SWR-aligned rasters of example neurons (top), and corresponding average firing rates (bottom). Neurons in columns 1 and 2 showed strong excitation during SWRs (SWR-excited). Neurons in columns 3 and 4 were SWR-inhibited, and the neuron in column 5 was SWR-unmodulated (p's < 10^{-3} for modulated neurons; p = 0.4 for unmodulated neuron.

(B) SWR-triggered mean firing of all PFC units. Each row shows the z-scored mean SWR-triggered firing of one neuron. Neurons are ordered by their firing amplitude in a 0–200 ms window after SWR onset. Arrows mark the location of example neurons shown in (A).

(C) *Left*, Population PSTHs for CA1, PFC SWR-excited and PFC SWR-inhibited cell populations sorted by the timing of the peak or trough in the SWR-modulated PSTH. *Middle*, Same plots for neurons recorded only on the W-track. *Right*, Same plots for neurons recorded only on the Y-track.

(D) Population-averaged SWR-triggered PSTHs for CA1, PFC SWR-excited and SWR-inhibited populations. Shaded areas are s.e.m.

(E) *Left* Distribution of the time of the peak of the SWR response for the populations in (D). *Right* Distribution of the onset rise / fall time of the SWR response for the populations in (D). Both SWR-excited and SWR-inhibited PFC populations had significantly later peaks/troughs and longer time to rise compared to the CA1 population (p's < 0.001, rank-sum test).

(F) Mean standardized cross-covariance during SWRs for CA1 vs. SWR-excited pairs (n = 393), and CA1 vs. SWR-inhibited pairs (n = 320). Insets show area around peaks.

See also Table S2.

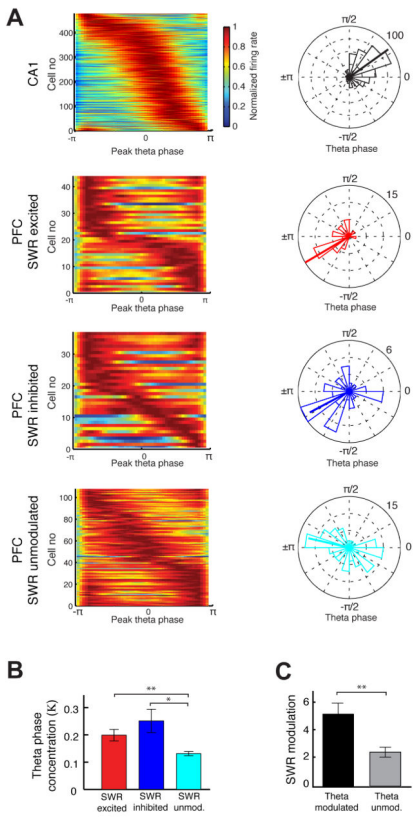

Figure 4. Phase Locking of PFC Neurons to Hippocampal Theta

(A) *Left* Normalized firing rates as a function of CA1 theta phase. Each row in the color plot shows the normalized theta-phase aligned histogram of a neuron with significant phase-locking. The rows are sorted by peak theta phase of each neuron. *Right* Polar plots quantifying the distribution of peak phases for the populations shown on left. Numbers on top right indicate radius of the plot, the scale for number of neurons.

(B) Average concentration parameter (κ) quantifying strength of phase locking (*$p < 0.01$, **$p < 0.001$, rank-sum test).

(C) Average SWR modulation in theta modulated and theta unmodulated PFC populations (**$p < 0.01$, rank-sum test).

See also Table S3.

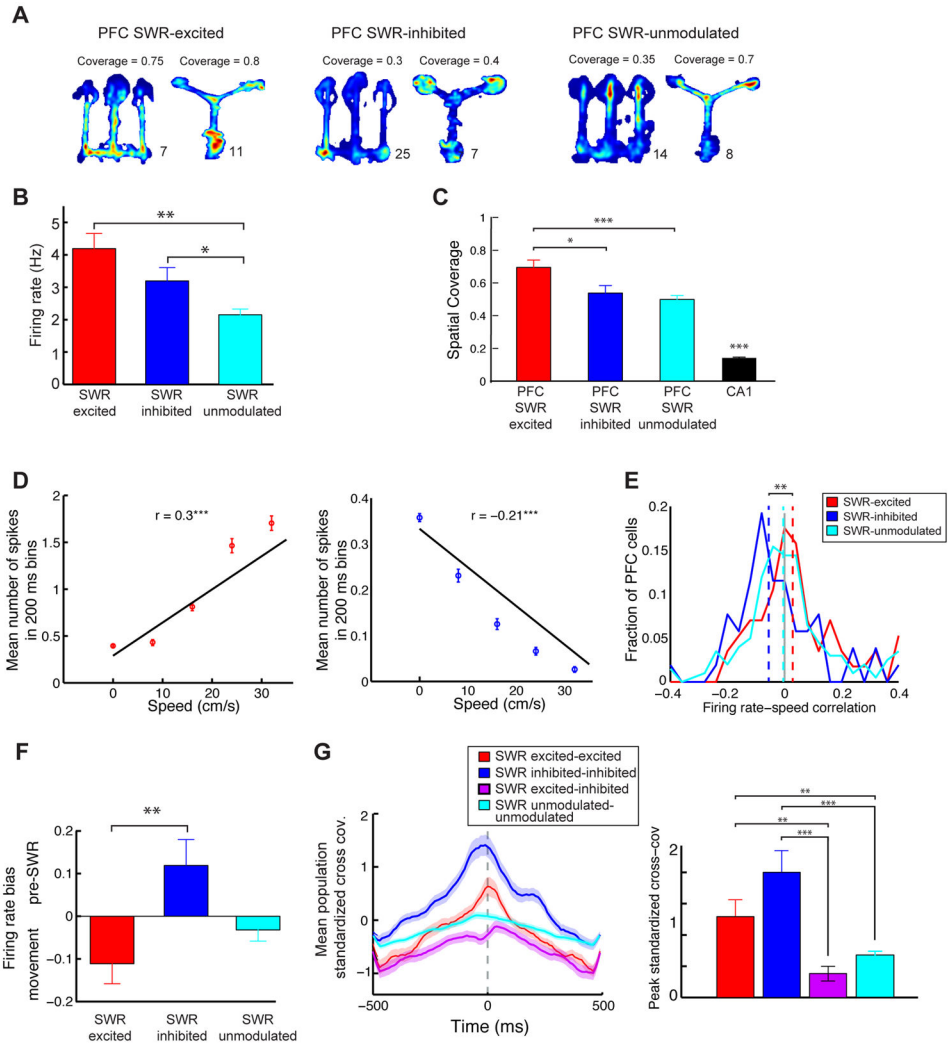

Figure 5. Evidence for Distinct Functional PFC Populations Related to SWR-Modulation

(A) Example occupancy normalized spatial firing rate maps of PFC cells with varying degrees of spatial coverage of the environment. Numbers in the lower right of each color plot indicate the firing rate corresponding to red.

(B) Mean firing rates of SWR-excited, SWR-inhibited and SWR-unmodulated PFC populations (*$p < 0.01$, **$p< 0.001$, rank-sum test).

(C) Spatial coverage of neurons. The CA1 population is also shown for comparison, and has significantly lower coverage than all the PFC populations ($p< 10^{-4}$, rank-sum test; *$p< 0.01$, ***$p< 10^{-4}$, rank-sum test).

(D) Firing rate and speed correlation for a SWR-excited PFC cell (*left*, positively correlated) and SWR-inhibited PFC cell (*right*, negatively correlated) ***$p< 0.0001$, regression test.

(E) Distribution of firing rate-speed correlations for the PFC populations. Overlaid are medians of distributions (**$p< 0.01$, rank-sum test).

(F) Firing rate modulation index quantifying difference in pre-SWR periods (−500 to −100 ms before SWR onset) and high-speed periods (> 10 cm/sec). Index varies between −1 to

+1, with +1 indicating firing only in the pre-SWR window and −1 indicating firing only during movement (**p< 0.01, rank-sum test).

(G) Standardized cross-covariance during theta periods for PFC pairs belonging to different SWR-modulation populations. *Left* average population cross-covariances. Shaded areas are s.e.m. *Right* Average peak of the cross-covariance for the populations (**p< 0.001, ***p< 10^{-4}, rank-sum test).

See also Figure S3.

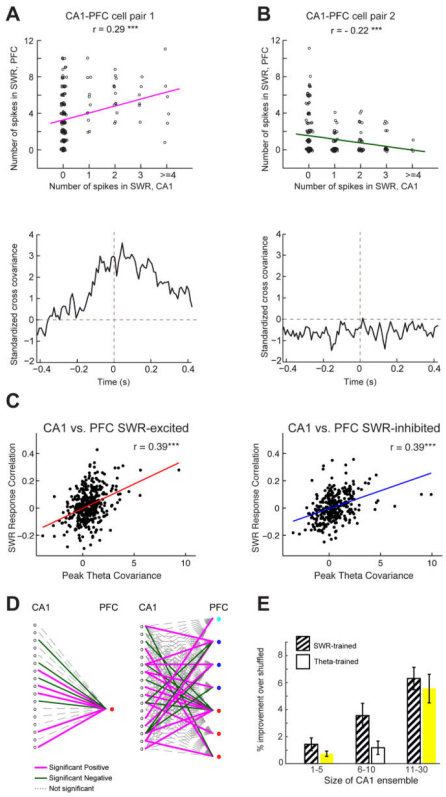

Figure 6. CA1-PFC Reactivation During Awake SWRs

(A) Top, number of spikes across all SWRs of one PFC neuron against number of spikes of a simultaneously recorded CA1 neuron. Spike counts were jittered for visualization only (Gaussian jitter with s.d. = 0.05 for x-axis, and s.d. = 0.1 for y-axis). Bottom, standardized cross-covariance of the neuronal pair during theta (r = 0.29, p = $4.5e^{-5}$***).

(B) Same as in a, for a pair with negative SWR-correlation and low theta cross-covariance (r = −0.22, p = 0.0006***).

(C) *Left* SWR correlation vs. theta cross-covariance for CA1 vs. SWR-excited PFC cells (n = 393 pairs; r = 0.39, $p < 10^{-4}$). *Right* SWR correlation vs. theta cross-covariance for CA1 vs. SWR-inhibited PFC cells (n = 320 pairs, r = 0.39, $p < 10^{-4}$).

(D) *Left* A GLM obtained for an example CA1 ensemble and PFC cell, where spiking of the CA1 ensemble during SWRs was used to predict spiking of the PFC cell during SWRs. Edges represent GLM beta coefficients. *Right* The network from the left embedded within a larger network that includes the other PFC cells recorded simultaneously. Red dots represent SWR-excited PFC cells, blue dots represent SWR-inhibited PFC cells and cyan dots represent SWR-unmodulated PFC cells.

(E) Cross-validated prediction for SWR-associated spiking of PFC SWR-modulated cells. Prediction is plotted as a function of the CA1 ensemble size. SWR-trained (striped bars) prediction performance increased with the size of the CA1 ensemble (1-way ANOVA, cell count group: $p< 10^{-4}$). Movement-trained (white bars) prediction performance also increased with the size of the CA1 ensemble (1-way ANOVA, cell count group: $p< 10^{-7}$). See also Figure S4.

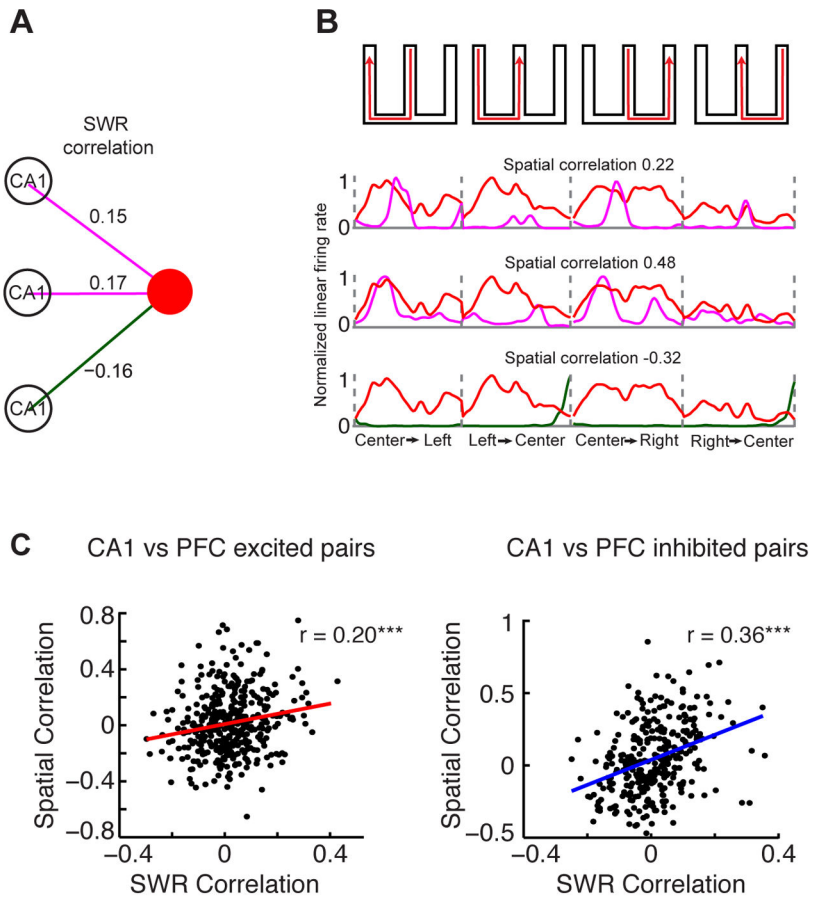

Figure 7. CA1-PFC Reactivation reflects Spatial Correlations

(A) Example PFC neuron and three simultaneously recorded CA1 neurons. The purple and green lines represent significant positive and negative SWR-correlations, respectively. The corresponding SWR correlation coefficients are shown above their respective lines.

(B) Normalized linear firing rate of the corresponding CA1 neurons from (A) for each of the W-track spatial trajectories, overlaid on the PFC firing rate in red. The spatial correlation coefficients for these CA1-PFC pairs are shown above their respective linear firing rate maps.

(C) Spatial correlation vs. SWR correlation for (*Left)* CA1 vs. SWR-excited PFC cells (n = 393 pairs, r = 0.2, $p < 10^{-3}$), and (*Right)* CA1 vs. SWR-inhibited PFC cells (n = 320 pairs; r = 0.36, $p < 10^{-4}$). The SWR-inhibited population had stronger correlations than SWR-excited population, $p < 0.01$, shuffle test, n = 1000).

See also Figures S5 and S6.

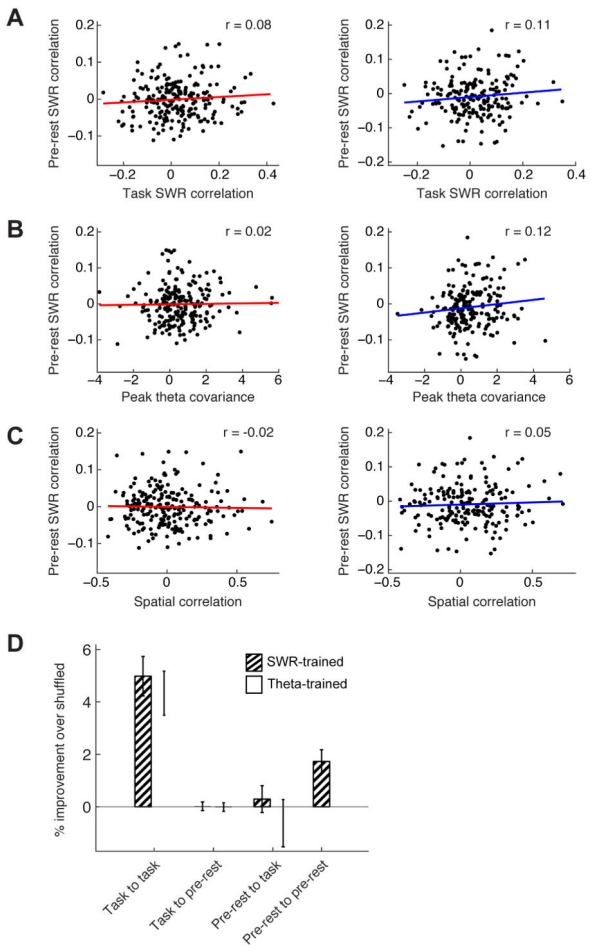

Figure 8. Task Related CA1-PFC Correlations are Not Present in Preceding Rest Periods

(A) SWR response correlation in pre-rest vs. task behavior for all CA1-PFC pairs recorded in both epochs for W-track behavior. (*Left*) CA1-PFC SWR excited pairs (n = 219, r = 0.08, p = 0.2). (*Right*) CA1-PFC SWR inhibited pairs (n = 196, r = 0.1, p > 0.1).

(B) SWR response correlation vs. peak theta cross-covariance during task behavior vs. during pre-rest periods. (*Left*) CA1-PFC SWR excited pairs (n = 219, r = 0.02, p > 0.8). (*Right*) CA1-PFC SWR inhibited pairs (n = 196, r = 0.12, p > 0.1).

(C) Pre-rest SWR response correlation vs. spatial correlation during behavior. (*Left*) CA1-PFC SWR excited pairs (n = 219, r = −0.02, p > 0.7). (*Right*) CA1-PFC SWR inhibited pairs (n = 196, r = 0.05, p > 0.5).

(D) Comparison of cross-validated GLM models for prediction of SWR-associated spiking of PFC cells using CA1 cell activity. Task to task: Behavior model to predict behavioral data (n = 38 PFC SWR-modulated cells). Task to pre-rest: Behavior model to predict pre-rest data (n = 24 cells). Prediction was significantly lower than run-to-run performance (SWR-trained: ranksum test, n = 38 vs. n = 24 cells, $p < 10^{-6}$; Theta-trained: $p < 10^{-5}$). Pre-rest to task: Pre-sleep model to predict behavioral data (n = 22 cells). Prediction was significantly lower than run-to-run performance (SWR-trained: ranksum test, n = 38 vs. n = 22 cells, $p < 10^{-6}$; Theta-trained: $p < 10^{-4}$). Pre-rest to pre-rest: Pre-rest model to predict pre-rest data (n

= 39 cells). Prediction was significantly higher than either of the two cross-epoch predictions (SWR-trained: ranksum test, n = 39 vs. n = 24 cells, $p < 0.01$; n = 39 vs. n = 22 cells, $p < 0.01$).

See also Figure S7.